Numerical simulations of photon acceleration occurring during the modulation of a long laser pulse in plasma

R. M. G. Trines, C. Murphy, P. A. Norreys
Central Laser Facility, STFC, Rutherford Appleton Laboratory, HSIC, Didcot, Oxon OX11 0QX, UK

J. T. Mendonça and L. O. Silva
GOLP/Instituto de Plasmas e Fusão Nuclear, Instituto Superior Técnico, Lisbon, Portugal

R. Bingham
Space Science and Technology Department, STFC, Rutherford Appleton Laboratory, HSIC, Didcot, Oxon OX11 0QX, UK

Contact | **raoul.trines@stfc.ac.uk**

Introduction

In laser-wakefield acceleration, the strong plasma wakefields are not only capable of accelerating electrons, but also of changing the frequency (energy) of the photons in the driving laser pulse [1–6]. For this concept to work, the laser frequency commonly needs to be much higher than the plasma frequency, so the space and time scales of the plasma perturbations are much larger than the photon wavelength and period. In this case, geometric optics can be used to describe the motion of the electromagnetic wave-packets as well as the influence of the plasma on this motion [6]. The action of the photons on the plasma can be described through the action of the ponderomotive force [4]. Experimental confirmation of photon acceleration by laser-induced wakefields was first reported by Murphy, Trines *et al.* [7].

In this paper, we will investigate the role of photon acceleration in the modulational instability of a laser beam in a plasma. The modulational instability is an effect that tends to break up an initially uniform electromagnetic (EM) wave propagating through a plasma, and can be understood in terms of the ponderomotive force. If the EM wave amplitude has a maximum at some point, then the ponderomotive force tends to push plasma away from that point and to produce a region of reduced density. The variation with density of the plasma refractive index is such that the EM wave tends to be refracted towards regions of lower density, with the result that the original amplitude perturbation is enhanced. If the break-up is in the direction of propagation, it is called the modulational instability, while a transverse break-up is called the filamentation instability. Detailed information on the modulational instability can be found in Refs. [13–15].

From the work by Silva *et al.* [3, 4] and Mendonça [6], it follows that the back action of the laser's ponderomotive force will change the momentum (wave number) and energy (frequency) of the laser's photons themselves. Thus, the modulational instability will not only change the envelope of the laser beam in real space, but also its Fourier spectrum. In particular, the spectrum will broaden and a series of peaks will emerge on that are separated by much less than the plasma frequency (so they can be distinguished from mere stimulated Raman scattering), while ionization blueshift would shift the spectrum as a whole (cf. Koga *et al.* [12]) rather than modulating it. The extent of the spectral broadening and the separation of the peaks are a measure of the amplitude of the laser-driven wakefield, and can be used to diagnose this wakefield. In this paper we will discuss the spectral modulations of the driving laser pulse itself; as an alternative (e.g. when the driving pulse is too short to be properly modulated) a long, low-intensity 'witness' pulse can be launched simultaneously with the driving pulse, and the wakefield can be studied through modulations of this witness pulse.

Theory

The modulational instability causes the fundamental spectral peak of the laser to split into several narrower peaks, having a mutual separation much smaller than ω_p. It will have the same effect on any (anti-)Stokes peaks in the spectrum, although we did not study this in our experiment. This distinguishes the modulational instability from e.g. stimulated Raman scattering, which only produces discrete peaks separated by the plasma frequency ω_p. This can be understood as follows.

Consider a laser EM field $E = E_0 \exp i(k_0 x - \omega_0 t)$ propagating through a plasma slab of thickness s and density n_0, accompanied by a co-propagating plasma density perturbation $\delta n = \delta n_0 \cos(k_p x - \omega_p t)$ with $k_p = k_0\omega_p/\omega_0$. The dispersion relation of the laser wave is given by:

$$D \equiv \omega^2 - e^2k^2 - (e^2/\varepsilon_0 m_e)(n/\gamma) = 0, \qquad (1)$$

where γ denotes the relativistic Lorentz factor due to plasma electron motion and other symbols have their usual meaning. After traversing the plasma slab, the laser frequency will have been modulated periodically: $\omega = \omega_0 + \delta\omega$, with (using ray tracing theory):

$$\delta\omega \approx \frac{d\omega}{dt}\frac{kg}{\omega} = \frac{\vartheta D/\partial t}{\vartheta D/\partial\omega}\frac{k8}{\omega}$$
$$\approx \frac{1}{2\omega_0}\frac{e^2}{\varepsilon_0\gamma m_e}\frac{\vartheta n}{\vartheta t}\frac{k_0 8}{\omega_0} = -\delta\omega_0 \sin(k_p x - \omega_p t),$$

with $\delta\omega_0/\omega_p = k_0 s\omega_p^2/(2\omega_0^2)\delta n_0/n_0$. Using standard series expansions[20], we find that, after passage through the plasma slab, the modulated laser field takes the form:

$$E \approx E_0 \exp i(k_0 x - [\omega_0 - \delta\omega_0 \sin(k_p x - \omega_p t)]t)$$

$$= E_0 \exp i(k_0 x - \omega_0 t) \sum_{l\approx-\infty}^{\infty} J_l(t\delta\omega_0) \exp il(k_p x - \omega_p t).$$

For fixed x, we find that the modulated frequency spectrum of E now contains peaks at $\omega_0 \pm l\omega_p \pm \delta\omega_0$, $l = 0, 1, 2, \ldots$ Note that the frequency shifts of $\pm\delta\omega_0$ are a direct consequence of the fact that the Bessel functions J_l are approximately periodic with period 2π. While the (anti-)Stokes peaks at $\omega_0 \pm l\omega_p$ will also occur for 'classical' Raman scattering of a monochromatic beam, the additional contribution of $\pm\delta\omega_0$ is typical for a beam that is frequency-modulated by photon acceleration. These modulations will be most visible around the fundamental peak of the laser spectrum, and our experiments will also concentrate on the study of this peak.

In realistic situations, the density perturbation will not have constant amplitude along the length of the laser pulse; instead, the perturbation will be driven resonantly by the modulated pulse and its amplitude will increase from the front to the back of the pulse. Therefore, each period of the density perturbation covered by the pulse will add contributions at $\pm\delta\omega_0$ for a different value of $\delta\omega_0$. This will cause the fundamental laser peak to separate into a series of narrow peaks separated by $\delta\omega_0 << \omega_p$, This separation increases with increasing plasma density, as $\delta\omega_0 \sim \omega_p \sim n_0^{1/2}$. By determining the background density n_0 and the thickness of the plasma slab s, it can be worked out what the wakefield amplitude must have been. Therefore, study of the spectral modulations induced by photon acceleration of a long laser pulse may eventually yield a single-shot wakefield diagnostic.

Simulations

We have performed simulations to match the experiments, using a photon kinetic numerical code. In this code, the individual electromagnetic wave modes that make up the finite-length, finite-bandwidth laser pulse are treated as particles, while the electron plasma is treated as a fluid. A detailed description of the model can be found elsewhere[7,23]. Simulation parameters were as follows: a 45 fs, bandwidth limited pulse with $\lambda = 800$ nm was chirped (lowest frequencies first) and stretched to a FWHM of 180 fs and a peak amplitude of $eA/(m_e c) = 0.4$. The plasma density n_0 was 2, 4, 8 or 16×10^{18} cm^{-3} giving $\omega_0/\omega_p = 29$, 4, 20.9, 14.9 or 10.4 respectively. For $n_0 = 1.6 \times 10^{19}$ cm^{-3}, a snapshot was taken after $\omega_p t = 7200$, or about 9 mm propagation length.

Simulation results are shown in figures 1 ($n_0 = 1.6 \times 10^{19}$ cm^{-3} only) and 2 (all densities). The left frame of Figure 1 shows the frequency spectrum of the transverse EM field (laser field) after 9 mm of propagation. It can clearly be seen that the fundamental peak of the spectrum has separated into several peaks. The corresponding photon distribution as a function of x and k can be seen in the right frame. The photon distribution has been modulated by the underlying plasma wave, and various populations of photons can be seen both above and below the original wave number $k_0 = 10.4 * k_p$. These photon populations are responsible for the peaks in the spectrum: where the original photon distribution consisted of only one population which caused only one peak, the final distribution consists of a number of photon populations that have been accelerated to wave numbers different from k_0 and thus contribute individual peaks to the laser spectrum.

The main features of the laser spectrum in figure 1 are the distinctive peaks separated by about ω_p. These are the standard (anti-)Stokes peak corresponding to classical Raman forward scattering, whose emergence has been

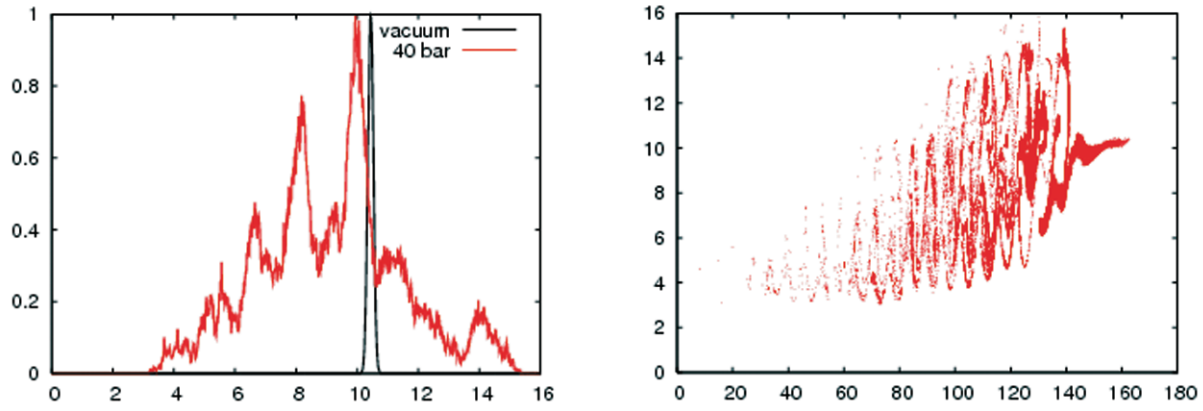

Figure 1. Simulation results for the modulational instability of a long laser pulse. Depicted are the transmission spectrum (top, intensity versus ω/ω_p) and the distribution of the laser's photons in (x, k)-space (bottom, ck/ω_p versus $\omega_p x/c$) after the laser pulse propagated through the plasma for 9 mm. The transmission spectrum shows large peaks separated by ω_p, indicating that the modulational instability is fully developed to the point of saturation. The photon distribution displays extensive phase mixing of the photons, most of which have already completed several closed orbits in (x, k)-space by this time. The accumulation of photons at the 'top' and 'bottom' of such closed orbits leads to the peaks in the transmission spectrum.

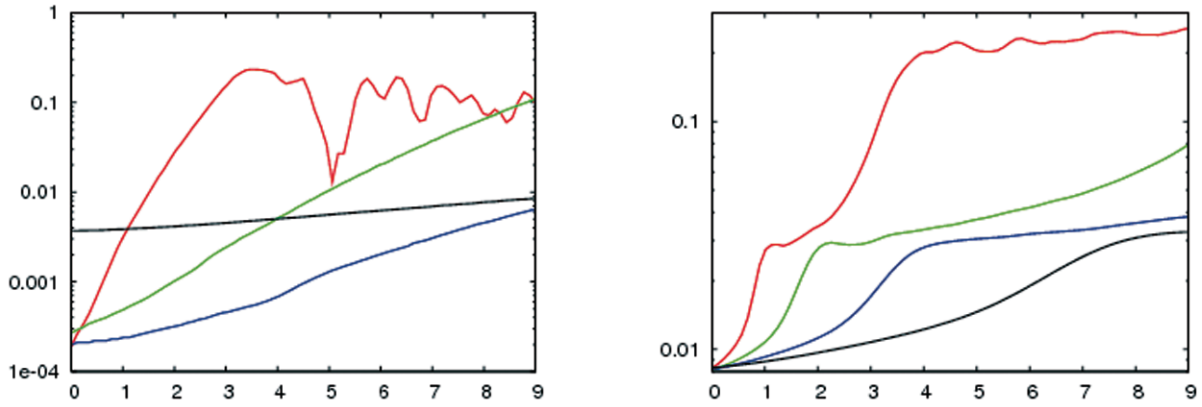

Figure 2. Simulation results for the modulational instability of a long laser pulse. Depicted are the amplitude of the longitudinal electric field $eE/(m_e\omega_p c)$ (top) and the width of the laser's spectrum $\delta\omega/\omega_0$ (bottom) versus propagation distance in mm, for background electron densities of $n_0 = 2$ (black), 4 (blue), 8 (green) and 16×10^{18} cm^{-3} (red). It is found that both quantities, in particular the wakefield amplitude, grow exponentially once the modulational takes off properly. The growth time has been found to scale with $1/\omega_p^3$ due to the effect of finite pulse length on the development of the modulational instability. For the highest density, it is found that the modulational instability saturates after about 4 mm of propagation.

predicted above. Their presence indicates that the modulational instability is well developed at the time the snapshot was taken and saturation has already set in. This is confirmed by the right frame of figure 1, which shows the position and wave number of the laser pulse's photons. Almost all photons have shifted considerably with respect to their original wave number k_0, and have completed at least one turn along a closed orbit in (x, k)-space. Extensive phase mixing has occurred and the spectral broadening has mostly saturated.

Although the narrow peaks at $\omega_0 \pm \delta\omega$ are just about visible in the simulated spectra at early times, it is easier to obtain information about $\delta\omega$ by simply looking at the full width of the laser spectrum before the emergence of the (anti-)Stokes peaks at $\omega_0 \pm 1*\omega_p$. To illustrate this, both the width of the frequency spectrum and the amplitude of the longitudinal electrostatic field E_x (the wakefield) have been plotted versus propagation distance in figure 2 for simulated densities of $n_0 = 2$, 4, 8 and 16×10^{18} cm^{-3}. A careful analysis shows that the growth time of both the spectral width and the wakefield is proportional to $1/\omega_p^3$. This is different from the usual expression of $1/\omega_p^{3/2}$ or $1/\omega_p^2$ [22], but one should bear in mind that these results were calculated for laser beams of infinite length. Using a pulse of fixed, finite length introduces a stronger dependence of the growth time on ω_p, because the pulse length increases relative to the plasma period for an increase in ω_p. Since the spectral width grows at a rate equal to the wakefield amplitude, this proves that an analysis of the spectral width after the interaction will yield the peak wakefield amplitude reached during the interaction. Even better results will be obtained when the modulation of a low-intensity 'witness' laser pulse is studied rather than that of the driving pulse, as there will be much less evolution of the wakefield under the witness pulse in that case, which renders it easier to relate the spectral broadening back to the wakefield amplitude.

Conclusions

We have studied the role of photon acceleration in the modulational instability of a long laser pulse (180 fs) with an underdense plasma. The modulational instability causes the laser pulse envelope to be modulated on the length scale of the laser-driven plasma wave, and it has been predicted that the plasma wave will also periodically modulate the laser frequency.

We have developed an analytic model for the spectral modulations that result from a periodic acceleration/deceleration of the laser's photon population. This model predicts that the fundamental spectral peak (and the Stokes satellites, which we did not study however) will split into two peaks with frequency $\omega = \omega_0 \pm \delta\omega$ with $\delta\omega_0/\omega_p = k_0 s\omega_p^2/(2\omega_0^2)\delta n_0/n_0$, s is the thickness of the plasma slab and δn_0 is the plasma wave amplitude. Since the plasma wave amplitude will grow throughout the laser pulse, each plasma period will contribute its own pair of spectral peaks at a different value of $\delta\omega$, leading to the generation of a number of narrow peaks, separated by considerably less than the plasma frequency.

For a maximum separation of up to 15 nm, as seen in a recent experiment [23], we have $\delta\omega/\omega_p = (\omega_0/\omega_p)(\delta\lambda/\lambda_0) = 0.2$, and a gas jet of about 3 mm wide will give us a density perturbation of $\delta n/n_0 = 0.016$. This value is in line with expectations for the case of a long, low-intensity laser pulse interacting with a tenuous plasma, and confirms the value of photon acceleration as a wakefield diagnostic.

Photon kinetic simulations show the separation of the fundamental peak into secondary peaks, as predicted by the theory and observed in the experiment. The simulations don't contain an ionisation model and don't exhibit an overall blueshift of the spectrum. This confirms the notion that a shift of the spectrum as a whole is caused by ionisation blueshift, while modulations of the spectrum are caused by wakefield-driven photon acceleration.

Acknowledgements

One of the authors (RT) would like to thank T. Katsouleas for valuable comments. This work was supported by the STFC Accelerator Science and Technology Centre.

References

1. S. C. Wilks, J. M. Dawson, W. B. Mori, T. Katsouleas, and M. E. Jones, *Phys. Rev. Lett*. **62**, 2600 (1989).
2. J. M. Dias, L. O. Silva and J. T. Mendonça, *Phys. Rev. ST Accel. Beams* **1**, 031301 (1999).
3. J. T. Mendonça and L. O. Silva, *Phys. Rev. E* **49**, 3520 (1994).
4. L. O. Silva, R. Bingham, J. M. Dawson, and W. B. Mori, *Phys. Rev. E* **59**, 2273 (1999).
5. L. O. Silva and J. T. Mendonça, *Opt. Commun.* **196**, 285 (2001).
6. J. T. Mendonça, *Theory of Photon Acceleration* (Institute of Physics Publishing, Bristol 2001).
7. C. D. Murphy, R. Trines, *et al*., *Phys. Plasmas* **13**, 033108 (2006).
8. R. L. Savage, C. Joshi and W. B. Mori Phys. *Rev. Lett.* **68**, 946 (1992).
9. W. M. Wood, C. W. Siders and M. C. Downer, *Phys. Rev. Lett.* **67**, 3523 (1991).
10. J. M. Dias, C. Stenz, N. Lopes, X. Badiche, F. Blasco, A. Dos Santos, L. Oliveira e Silva, A. Mysyrowicz, A. Antonetti and J. T. Mendonça, *Phys. Rev. Lett.* **78**, 4773 (1997).
11. N. C. Lopes, G. Figueira, J. M. Dias, L. O. Silva, J. T. Mendonça, Ph. Balcou, G. Rey and C. Stenz, *Europhys. Lett.* **66**, 371, (2004).
12. J. K. Koga, N. Naumova, M. Kando, L. N. Tsintsadze, K. Nakajima, S. V. Bulanov, H. Dewa, H. Kotaki and T. Tajima, *Phys. Plasmas* **7**, 5223 (2000).
13. R. A. Cairns, *Proc. SUSSP* **24**, 1 (1982).
14. K. Nishikawa, *in Advances in Plasma Physics* **6**, ed. A. Simon and W. B. Thomson (Wiley, 1976).
15. R. Bingham and C. N. Lashmore-Davies, *Plasma Physics* [*Plasma Phys. Contr. Fusion*] **21**, 433 (1979).
16. N. H. Matlis, S. Reed, S. S. Bulanov, *et al*., *Nature Physics* **2**, 749 (2006).
17. J. P. Geindre *et al*., *Opt Lett.* **19**, 1997 (1994).
18. J. R. Marquès, J. P. Geindre, F. Amiranoff, P. Audebert, J. C. Gauthier, A. Antonetti and G. Grillon, *Phys. Rev. Lett*. **76**, 3566 (1996).
19. C. W. Siders, S. P. Le Blanc, D. Fisher, T. Tajima, M. C. Downer, A. Babine, A. Stepanov and A. Sergeev, *Phys. Rev. Lett*. **76**, 3570 (1996).
20. M. Abramowitz and I. A. Stegun, *Handbook of Mathematical Functions with Formulas, Graphs, and Mathematical Tables* (Dover, New York, 1964).
21. C. J. Hooker *et al*., *Journal de Physique IV* **133**, 673 (2006).
22. C. J. McKinstrie and R. Bingham, *Phys. Fluids B* **4**, 2626 (1992).
23. R. Trines, C. Murphy, *et al*., *Plasma Phys. Contr. Fusion*, in press (2008).